



Modified-sorbents for acetone adsorption: Application in ethylene polymerization process

Maria Angélica C. Gollmann^a, Larissa B. Capeletti^a, Márcia S.L. Miranda^b, João H.Z. dos Santos^{a,*}

^a Instituto de Química, UFRGS, Av. Bento Gonçalves 9500, Porto Alegre 91501-970, Brazil

^b Braskem S.A., III Pólo Petroquímico, Via Oeste, Lote 05, Triunfo 95853-000, Brazil

ARTICLE INFO

Article history:

Received 30 August 2008

Received in revised form 3 November 2008

Accepted 14 November 2008

Keywords:

Adsorption

Poison

Ziegler-Natta catalyst

Chrysotile

Polyethylene

ABSTRACT

Ziegler-Natta catalysts are commonly employed in alfa-olefin (co)polymerization. Such systems are extremely sensitive to some organic compounds, which may act as poison, reducing polymer productivity. Among them, oxygenated compounds such as acetone can cause catalyst deactivation. In the present study, silica and chrysotile, in their pure form and after chemical modification with Cu and Ag, were characterized by a series of volumetric, spectroscopic and microscopic techniques. The results are discussed in terms of silanol group density, Lewis acid centers introduced by the metal and textural properties of the support. The resulting sorbents were evaluated in the adsorption of acetone from cyclohexane. Solvent containing acetone was percolated through the investigated sorbents and evaluated in the polymerization of ethylene using Ziegler-Natta catalysts. The best results in catalyst activity were observed in the case of silica or chrysotile modified with Cu.

© 2008 Elsevier B.V. All rights reserved.

1. Introduction

The term Ziegler-Natta catalyst encompasses a great variety of catalytic systems based on transition metals that are capable of polymerizing and co-polymerizing α -olefins and dienes. There are numerous polymer grades produced by Ziegler-Natta catalysts, such as high-density polyethylene (HDPE), low-density polyethylene (LDPE), low linear density polyethylene (LLDPE), and polypropylene (PP), to mention a few [1]. Currently, polyethylene production reaches 75.2 million tons a year, with predicted expansion to about 100 million tons in 2010 [2].

Nevertheless, as in any catalyst process, poisoning is an important issue of investigation [3–5]. Specifically, in the case of the titanium-based Ziegler-Natta ($\text{TiCl}_4/\text{MgCl}_2$) polymerization catalysts, such systems are strongly inhibited by alcohol, organic amines and sulfites, as shown by Eley et al. [6], Ballard et al. [7], Grayson and McDaniel [8] and Vizen et al. [9]. For these catalysts, traces of oxygenated compounds in the parts per billion (ppb) level are enough to engender significant loss of catalytic activity, because they can compete with ethylene for the Ti active site. Chlorine mobility in titanium chlorides has also been modeled as potential responsible for Ziegler-Natta catalyst deactivation [10]. These poisons can be indirectly introduced in the polymerization process by the solvent or by the feed stocks.

In order to avoid such problems, adsorbents have shown to be an economical way to remove contaminants from industrial solvents. For these processes, there are adsorbent materials such as silica, alumina and zeolites which are used industrially for the purification of solvents [11]. In recent years, other minerals in their natural or modified forms have been investigated as alternative potential adsorbents. Examples of the use as adsorbents of chrysotile [12] and kaolin [13] have been recently reported in the literature.

In the present paper, we report the use of chrysotile, native and modified with Ag and Cu, for the adsorption of acetone from cyclohexane, which is the solvent usually employed in the polymerization process. For comparative purposes, silica-based materials were modified with the same metals. The modification of such materials with Ag and Cu (Lewis acid centers) represents an attempt to increase the interaction of acetone with the adsorbent materials, and therefore reduce the poison content in the solvent.

2. Experimental

2.1. Chemicals

All employed chemicals were analytical reagent grade. For adsorption studies, the solutions were prepared using acetone (Mallinckrodt, HPLC) and cyclohexane (VETEC). Silica (provided by Braskem, Camaçari, Brazil) was used as received. Chrysotile (generously donated by SAMA, Mineração de Amianto Ltda, mined in Uruaçu, Brazil) was used in its native form and also after acid treatment.

* Corresponding author. Tel.: +55 51 3308 7238; fax: +55 51 3308 7304.

E-mail address: jhzds@iq.ufrgs.br (J.H.Z. dos Santos).

For the polymerization experiments, titanium tetrachloride (Merck), acetone and diethylaluminium chloride toluene solution (DEAC) were used without purification. Cyclohexane and toluene were purified by distillation on metallic sodium and benzophenone. Silica Grace 948 ($255\text{ m}^2\text{ g}^{-1}$), employed for the preparation of Ziegler-Natta catalyst, was activated under vacuum ($P < 10^{-4}$ mbar) for 16 h at 110°C . The support was cooled to room temperature under dynamic vacuum and stored under dried argon.

2.2. Adsorbent modification

2.2.1. Acid treatment

Leached chrysotile was prepared by treating natural chrysotile (ca. 30 g) with hydrochloric acid solution ($1000.0\text{ mL}-5.0\text{ mol L}^{-1}$), following a previously reported protocol [14]. The suspension was stirred for 48 h at room temperature. Then, it was filtrated and washed abundantly with water, yielding 15.0 g of product.

2.2.2. Chemical modification of silica and chrysotile

Silica (initially heated at 110°C for 8 h), chrysotile or leached chrysotile was treated with CuCl_2 or AgNO_3 aqueous solutions (5–50 wt %) for 4 h at room temperature. Then, the solvent was removed under heating and the resulting material was calcinated in air at 450°C for 8 h.

2.3. Adsorbent characterizations

2.3.1. X-ray diffraction spectroscopy (XRD)

The crystal structure and phase composition of the adsorbents were analyzed by powder X-ray diffraction, using a Rigaku X-ray diffractometer, model DMAX, with $\text{Cu K}\alpha$ radiation ($\lambda = 0.154178\text{ nm}$), at an accelerating voltage of 40 kV. Samples were analyzed as powders.

2.3.2. Scanning electron microscopy and energy-dispersive X-ray spectroscopy (SEM-EDX)

Grain morphology and metal distribution in the adsorbents was determined by a JEOL JSM-5800 scanning electron microscope. The samples were placed on an aluminum stub using double-sided adhesive tape and then coated with gold to avoid charging under the electron beam. An accelerating potential of 20 kV and a current of 18 mA were used during the measurement.

2.3.3. Nitrogen adsorption/desorption

Specific pore size distributions, surface area, and pore volume were calculated by the BET and BJH methods after nitrogen adsorption/desorption using a Gemini 2375 (Micromeritics) analyzer. Prior to the analysis, the samples were degassed at 150°C at 10^{-2} mbar for 4 h.

2.3.4. Diffuse reflectance infrared Fourier transmission spectroscopy (DRIFTS)

DRIFTS measurements were performed on a Bomem instrument, in reflectance mode. The spectra were obtained by coadding 32 scans at a spectral resolution of 4 cm^{-1} . Samples were analyzed as powders.

2.4. Equilibrium adsorption studies

A glass column ($L = 15\text{ cm}$; $\varnothing 0.5\text{ cm}$) was packed with adsorbent (10 g). The column was loaded with a solution (10 mL) of solvent contaminated with a known concentration of acetone (range 1–200 ppm) in cyclohexane that was percolated through the column under an equilibrium time of 20 min.

2.5. Polymerization

2.5.1. Synthesis of the supported Ziegler-Natta catalyst

In the preparation of the Ziegler-Natta catalyst, activated silica was impregnated with a toluene slurry containing MgCl_2 corresponding to 50 wt% $\text{MgCl}_2/\text{SiO}_2$, at 80°C for 30 min under reflux. Solvent was removed under vacuum and a TiCl_4 cyclohexane solution (corresponding to 3.0% Ti/SiO_2) was added. The resulting slurry was stirred for 1 h at room temperature and filtered through a fritted disk. More details are reported elsewhere [15].

2.5.2. Polymerization reactions

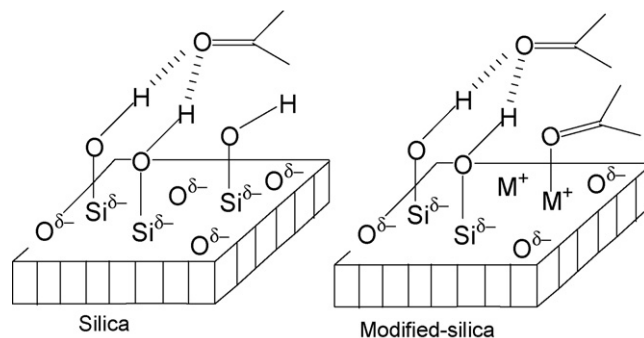
Ethylene polymerization reactions were performed in a 300 mL Pyrex glass reactor. The reactions were performed under Ar atmosphere using cyclohexane as the solvent (150 mL) in 1.6 atm of ethylene for 20 min at 60°C . DEAC was employed as the cocatalyst ($\text{Al}/\text{Ti} = 200$). For the non-supported TiCl_4 catalyst system the following conditions were employed: $[\text{M}] = 10^{-3}\text{ mol/L}$ and $\text{Al}/\text{Ti} = 5$, while for the supported ones: $[\text{M}] = 10^{-5}\text{ mol/L}$ and $\text{Al}/\text{Ti} = 200$. After distillation, cyclohexane was contaminated with acetone (0–80 ppm). In the reactions using adsorbents, the contaminated solvent (50 ppm) was percolated through the adsorbent (2.0 g) column under inert atmosphere and transferred into the reactor. Replicates in polymerization reactions were performed up to reach standard deviation lower than 6%. Catalyst activity was calculated taking into account the dried mass of the resulting polymer expressed in terms of metal present on the polymerization medium, either in terms of soluble catalyst or present on the supported catalyst.

2.5.3. Polymer characterization

The resulting polymers were characterized by differential scanning calorimetry (DSC). Polymer melting points (T_m) and crystallinities (X_c) were determined on a Thermal Analysis Instruments DSC-2010 calibrated with Indium, using a heating rate of $10^\circ\text{C min}^{-1}$ in the temperature range of $40\text{--}180^\circ\text{C}$. The heating cycles were performed twice, but only the second was taken into account, since the first cycle was influenced by the mechanical and thermal history of the samples. The samples (ca. $\approx 5\text{ mg}$) were put into an aluminum pan and hermetically sealed.

Table 1
Metal crystallite size of the chemically modified chrysotile and silica.

Sample	Particle size (nm)
LC Cu 50	10.1
LC Ag 50	10.4
S Cu 50	10.4
S Ag 50	10.3



Scheme 1. Interaction of carbonyl with (a) silica and (b) metal modified silica surface.

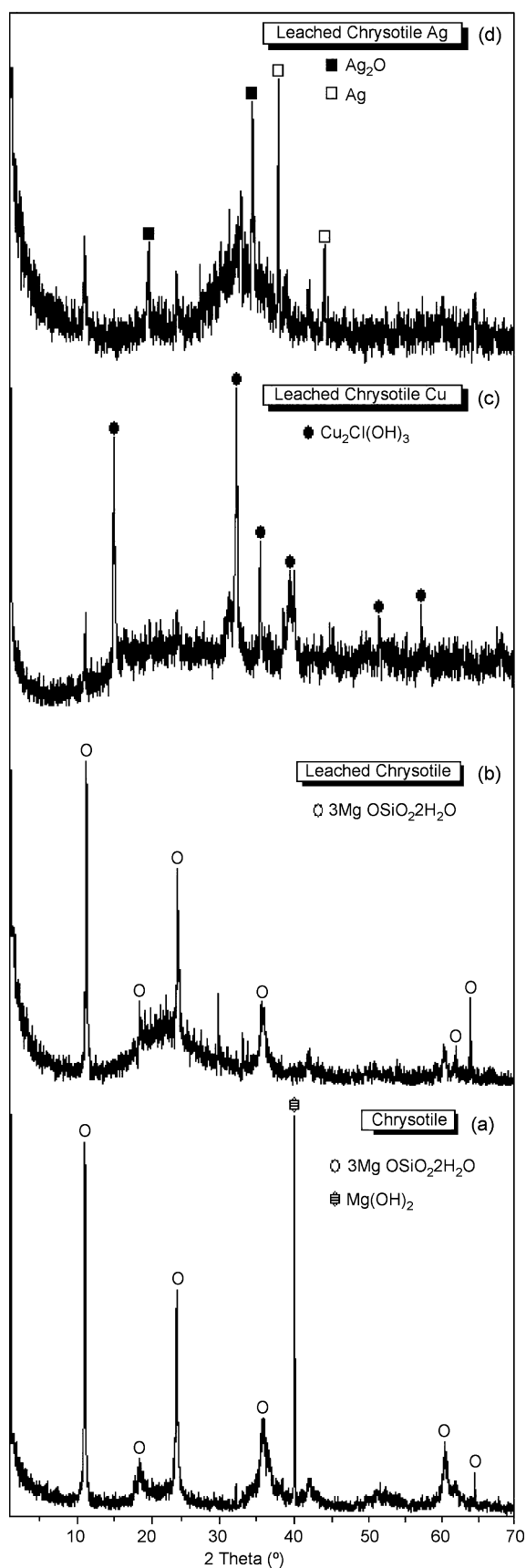


Fig. 1. X-ray diffraction patterns of chrysotile: (a) leached; (b) modified with Cu and (c) modified with Ag.

3. Results and discussion

The interaction of acetone with the silica surface has already been described by Schwarzenbach [16]. It takes place via a hydrogen bond between the oxygen from the carbonyl with the hydrogen from silanol groups. The introduction of a metal (M) on the surface engenders the formation of Lewis acid sites (M^+), which might also interact with the carbonyl group (Scheme 1).

The modification of silica and chrysotile with metals aims at improving the adsorption capacity of these supports by generating potential Lewis acid sites which are capable of interacting with acetone.

In the present study, silica and chrysotile, modified with different amounts of Ag and Cu were characterized by XRD, SEM and

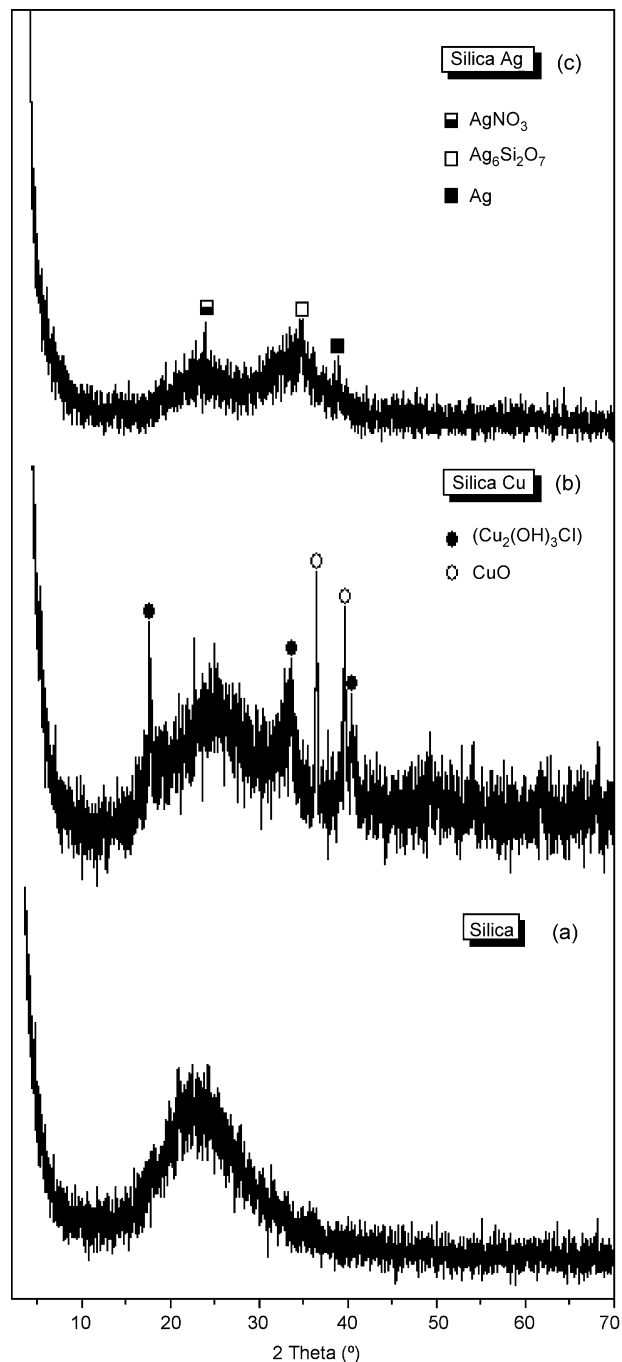


Fig. 2. X-ray diffraction patterns of silica: (a) pure; (b) modified with Cu and (c) modified with Ag.

nitrogen adsorption. In the following discussion, the labels contain the phase (S for silica, NC for native chrysotile and LC for leached chrysotile), the metal (Cu or Ag) and the metal content expressed in terms of percentage. So, for instance, LC Ag 5 indicates a leached chrysotile sorbent that was modified with 5 wt.% of Ag.

3.1. Adsorbent characterization

The external structure of natural chrysotile is mainly composed of magnesium mineral (brucite) as described in Refs. [17,18]. Normally, acid treatment removes this mineral and results in a nano-fibriform silica, which is completely amorphous [19]. The XRD patterns of native, leached and chemically modified chrysotiles are shown in Fig. 1.

In spectrum **a** of Fig. 1, the peaks at $2\theta=12.2$; 19.2 ; 24.3 ; 35.9 ; 61.8 and 64 are attributed to crystalline chrysotile. After acid leaching (spectrum **b**), the crystalline structure of chrysotile is maintained, but an amorphous structure can also be identified. The broad *halo* in the range of 20 – 30° (2θ) can be assigned to amorphous silica resulting from the acid treatment applied to the natural chrysotile. The observed disappearance of the peak centered at $2\theta=40^\circ$ is attributed to brucite. Spectrum **c** of Fig. 1 shows the results of copper-modified chrysotile. Signals centered at $2\theta=16.1$; 32.4 ; 36.6 ; 39.8 ; 50 and 57.1 are attributed to atacamita ($\text{Cu}_2\text{Cl}(\text{OH})_3$), as discussed by Larser and Noriega [20], Cai et al. [21] and Núñez et al. [22]. In the case of silver-modified chrysotile (spectrum **d** of Fig. 1), the peaks at $2\theta=20.9$ and 32.9 are attributed to silver oxide (Ag_2O), while those at $2\theta=34.8$ and 38.1 are attributed to metallic silver (Ag) [23,24].

For comparative purposes, silica was also chemically modified with Cu and Ag. The diffraction pattern of silica is characterized by a broad *halo* centered in the range of 18 – 30° (2θ), which indicates an amorphous structure (spectrum **a** in Fig. 2), according to Godec et al. [25]. After chemical modification, crystalline structures can be identified. According to spectrum **b** of Fig. 2, the signals at $2\theta=11.2$; 32.6 and 39.9 can be attributed to crystalline paratamamide ($\text{Cu}_2(\text{OH})_3\text{Cl}$) and those at $2\theta=35.6$ and 38.9 to crystalline tenorite (CuO). In Fig. 2c, the peaks observed at $2\theta=22.4$ can be assigned to AgNO_3 (starting product), that at $2\theta=34$ can be assigned to silver silicate ($\text{Ag}_6\text{Si}_2\text{O}_7$) and, finally, that at $2\theta=38.2$ corresponds to metallic silver (Ag).

The average crystallite size was estimated from the full width at half maximum (FWHM) of the XRD peaks assigned to the (200) $3\text{MgOSiO}_2\cdot 2\text{H}_2\text{O}$, (0 1 1) $\text{Cu}_2\text{Cl}(\text{OH})_3$ and (1 1 1) Ag, (0 0 2) CuO , (4 2 1) $\text{Ag}_6\text{Si}_2\text{O}_7$ phases, using Scherrer's equation. The calculated average crystallite sizes are presented in Table 1. Independent of the phase or of the element, particle metal size remained at ca. 10 nm.

Table 2

Textural properties of the adsorbents.

	Silica	Chrysotile	Leached chrysotile
S_{BET} (m^2/g)	646	23	294
D_p (\AA)	22	54	39
V_p (cm^3/g)	0.2	0.02	0.3

Table 3

Specific area (m^2/g) of adsorbents doped with metals determined by nitrogen adsorption and calculated by the BET method.

Metal content (wt.%)	Specific area ($\text{m}^2 \text{g}^{-1}$)	
	S	LC
	646	294
Cu (10)	578	136
Cu (50)	406	31
Ag (10)	454	27
Ag (50)	54	<10

Metal-modified silicas were also characterized by SEM. Fig. 3 illustrates the microstructure of S Cu 50 (a) and S Ag 50 (b). Among the investigated adsorbents, that resulting from the modification with Cu presents a homogeneously rough surface. In the case of S Ag 50, particles in the micrometer range can be observed.

Fig. 4 shows the micrographs of the LC (a) and after chemical modification: LC Cu (b) and LC Ag (c). Fig. 4a is characterized by long nanotubes and crystal-fiber bundles. When chrysotile is doped with Cu (Fig. 4b), the surface seems to be covered with particles, while in the case of Ag-modified chrysotile, particles seem to grow around the fibers.

In order to gain some information about their textural properties, the employed adsorbents were further characterized by N_2 adsorption. Table 2 shows the textural properties determined by nitrogen adsorption, calculated by the BET and the BJH methods [26].

According to Table 2, silica is the adsorbent with the highest specific area (S_{BET}), followed by LC. NC presents a very low specific area, but after the acid treatment there is a significant increase. The pore diameter (D_p) lay in the range of 20 – 60\AA , being higher in the case of natural chrysotile. The volume of the micropore (V_p) increased after acid treatment, being comparable to that of silica.

Table 3 shows the modification in specific areas after chemical treatment with Ag and Cu.

According to Table 3, the chemical modification of the adsorbents results in specific area loss, probably due to formation of metal deposition inside or in the opening of the pores. In the case

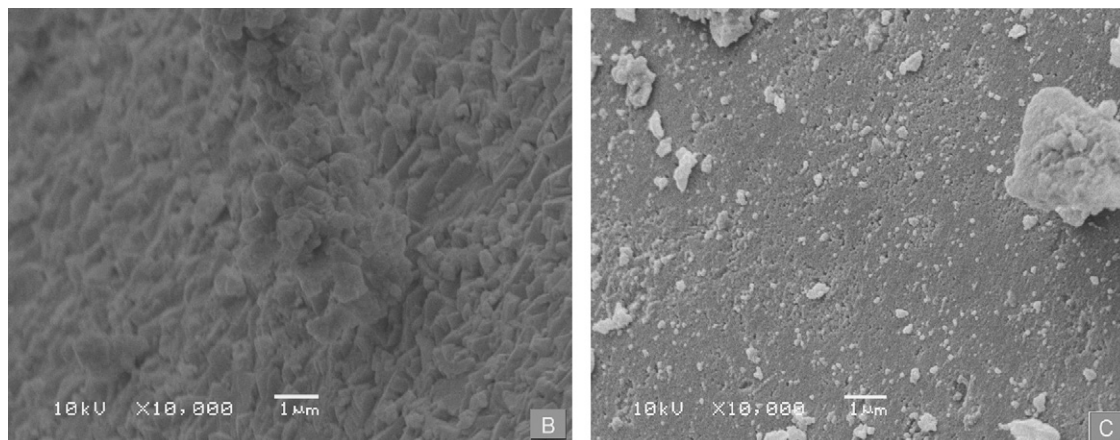


Fig. 3. Silica micrographs employed in adsorptions process, $10,000\times$: (a) doped with Cu (50%) and (b) doped with Ag (50%).

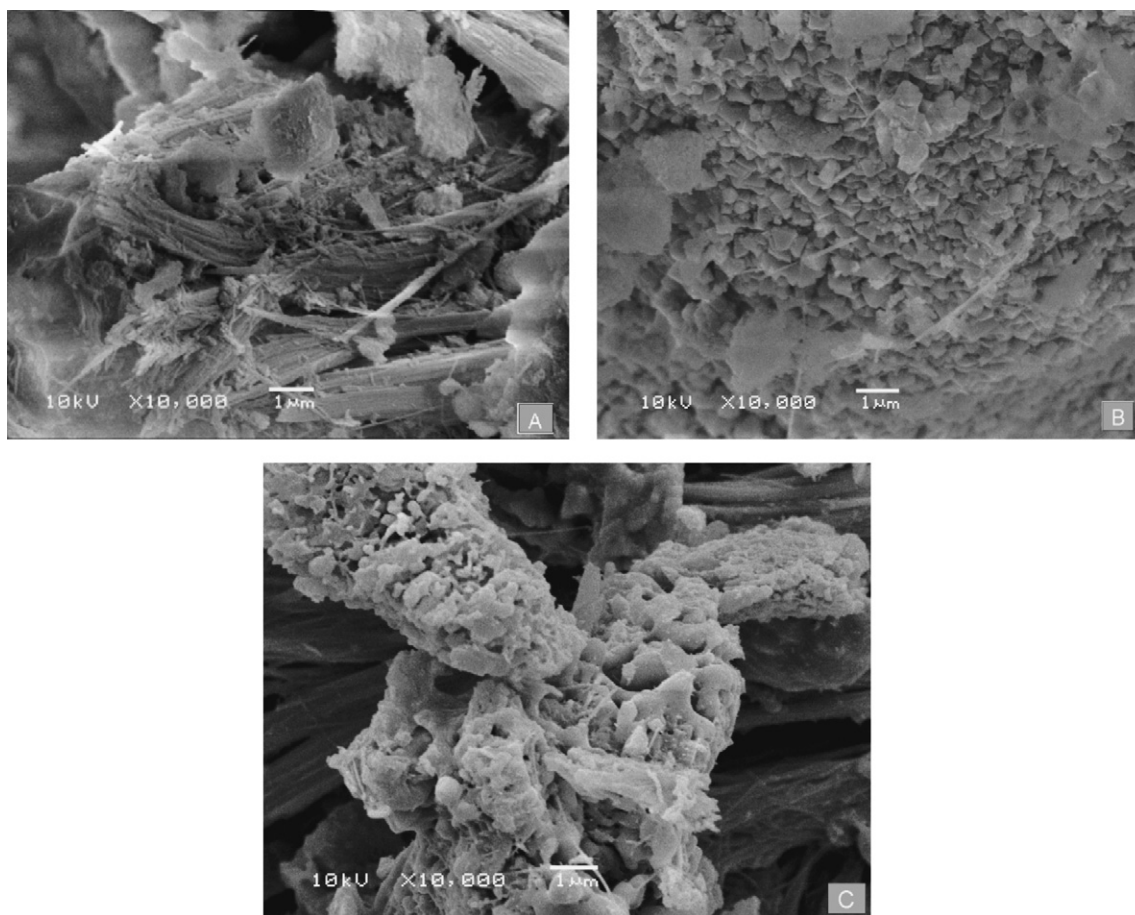


Fig. 4. Leached Chrysotile SEM images (22,000 \times): (a) pure, (b) modified with Cu (50 wt.%), and (c) modified with Ag (50 wt.%).

of silica modified with Ag, this loss is more accentuated than with Cu. In the leached chrysotile, the same behavior was observed. Alterations of D_p and V_p were not observed, suggesting that the deposition of metal must be occurring on the uppermost external surface of the grain adsorbent.

3.2. Acetone adsorption

Table 4 shows the percentage of acetone adsorption using modified chrysotile and silica. Data were expressed in terms of acetone adsorption capacity by adsorbents containing different amounts of M (Cu or Ag).

According to Table 4, the adsorbent capacity of pure leached chrysotile was higher than that of silica. The addition of metal in leached chrysotile, independent of the amount added, engendered a reduction in acetone adsorption capacity. For silica modified with Ag or Cu (10%), a positive effect was observed. When the amount of added metal increased (50%), the adsorption capacity was similar to that observed for bare silica.

Table 4

Acetone adsorption capacity on silica and leached chrysotile modified with Cu and Ag.

M (wt.%)	Acetone adsorption capacity (%)			
	LC Ag	LC Cu	S Ag	S Cu
0	96	96	73	73
10	51	46	90	93
50	58	49	75	72

Many phenomena might be involved in the acetone adsorption process, including the effect of the specific area and the nature of the surface sites and of the silanol concentration introduced by chemical modification. Attempts to elucidate the metal addition effect on the silanol concentration were performed by DRIFTS analysis (Fig. 5). For normalization of the signal, the area of the band centered at 3650 cm^{-1} (silanol groups) was divided by the area of the band at 1867 cm^{-1} (overtone Si–O–Si), taken as the internal standard, since it was invariant under the experimental conditions used in this analysis [27].

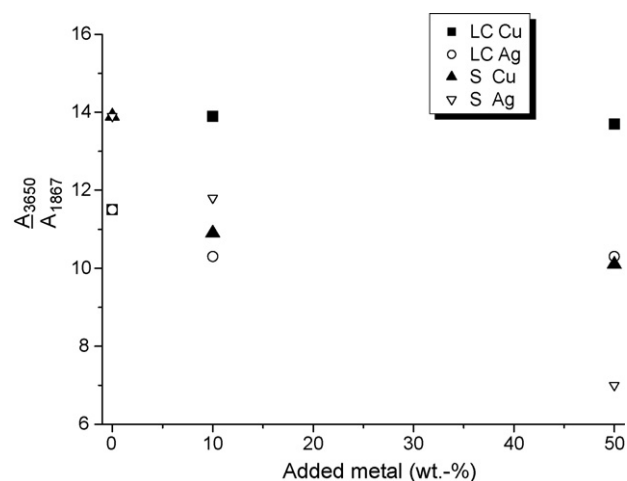


Fig. 5. Effect of metal loading on the silanol content.

Table 5
Acetone adsorption on silica and chrysotile, monitored by $\nu_{(C=O)}$. M = Cu or Ag.

Sorbent	Cu $\nu_{(C=O)}$ (cm^{-1})	Ag $\nu_{(C=O)}$ (cm^{-1})
S	1711	1711
S M 10	1697	1694
S M 50	1692	1691
LC	1707	1707
LC M 10	1696	1704
LC M 50	1692	1698

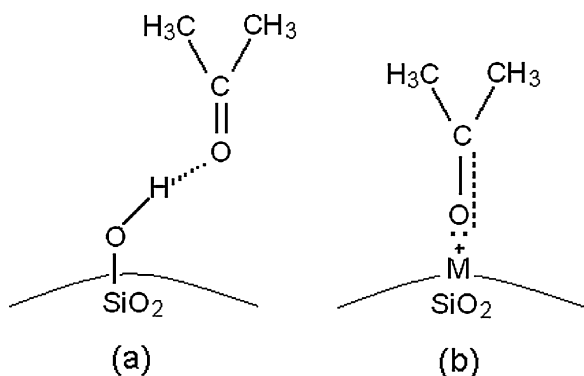
According to Fig. 5, for chrysotile there is a reduction in OH concentration, which shows to be practically independent of the added metal amount. Nevertheless, for silica the increase in metal concentration results in a significant reduction of silanol groups. This reduction is clear when the modification of silica is made with Ag. Then, as the metal content increases, the number of potential immobilization Lewis acid sites also increases. Nevertheless, for silica, metal modification engenders the reduction of silanol groups, which are also potential adsorption groups. Acetone adsorption on the silica surface modified with metals was also monitored through DRIFTS. The $\nu_{(C=O)}$ stretching for isolated acetone appears at 1737 cm^{-1} [28]. The stretching $\nu_{(C=O)}$ of acetone adsorbed on silica and on chrysotile is presented in Table 5.

Considering data for pure acetone ($\nu_{(C=O)} = 1737 \text{ cm}^{-1}$) and data presented in Table 5, it is observed that $\nu_{(C=O)}$ shifted to lower wavenumber values both in the case of silica and leached chrysotile. This shift of $\nu_{(C=O)}$ for lower wavenumbers suggests that the metal addition increases the acetone interaction with the adsorbent surface. There is a reduction in the bond order of the carbonyl in acetone, probably due to coordination onto the metallic center (Lewis acid sites), presented on the silica surface, as proposed in Scheme 2.

Evaluating all these factors, it seems that the OH concentration and the increase in Lewis acidity through the increase of silica metal loading are factors that compete between themselves. For low metal addition (10%), acetone adsorption capacity increases. However, when this amount of metal loading increases (50%), the reduction of OH groups on the surface is relatively significant, resulting in a decrease in acetone adsorption capacity of silica.

3.3. Catalyst activity and polymerization

In order to evaluate the acetone adsorption capacity of the investigated adsorbents, cyclohexane was contaminated with acetone (50 ppm) and percolated through the adsorbent materials. These solvents were used in the reaction of ethylene polymerization. Fig. 6 correlates the relative catalytic activity (%) in ethylene polymerization reactions for the different silica-based adsorbents.



Scheme 2. Bonding order of carbonyl group on (a) silica and (b) metal modified silica surface.

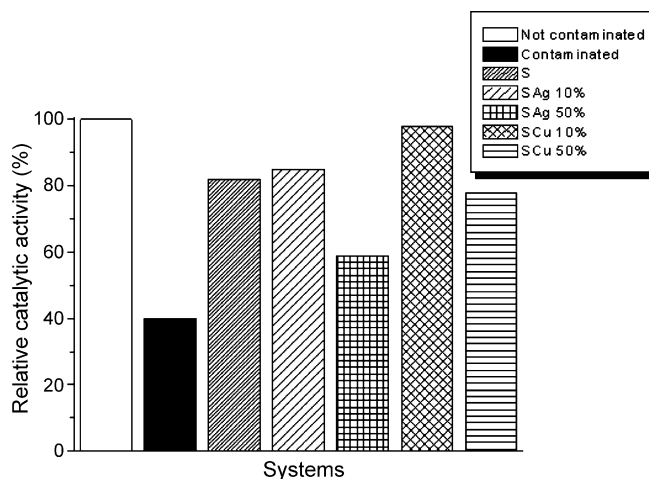


Fig. 6. Catalytic activity in the ethylene polymerization with $\text{TiCl}_4/\text{MgCl}_2$ catalyst, using cyclohexane contaminated with 50 ppm of acetone and percolated through chemically modified silicas.

The polymerization results displayed in Fig. 6 show that loading 10% metal for silica is more efficient than loading 50%. This confirms the results observed in acetone adsorption that demonstrated that 10% metal is better for this system. Moreover, as previously observed, the modification with Cu is more efficient than with Ag: for the modification of silica with 10% metal, 97% efficiency is obtained for Cu, as opposed to 83% for Ag. Bare silica (S) presents values of catalytic activity comparable with S Ag 10%. Therefore, modification with Ag does not seem to improve acetone retention on silica. Fig. 7 shows the relative catalytic activity (%) in polymerization reactions, using LC modified with Ag and Cu.

According to Fig. 7, the LC doped with 50% of Cu presents less loss of the catalytic activity. For Ag, the effect of impregnated metal in the loss of catalytic activity is practically non-existent: 78% efficiency for 10% metal and 75% for 50% Ag added. For Cu, the catalytic activity is comparable to the non-contaminated system (98% of efficiency). For polymerization reactions, pure LC was shown to be less efficient than LC modified with metals. Perhaps LC applied in polymerization reactions releases some poison for polymerization process. NC was also evaluated as an adsorbent for the solvent used in polymerization reactions. Results, in terms of relative catalytic activity in ethylene polymerizations with NC, are shown in Fig. 8.

NC has been previously evaluated for acetone adsorption and showed worse adsorption capacity in comparison to coal or alu-

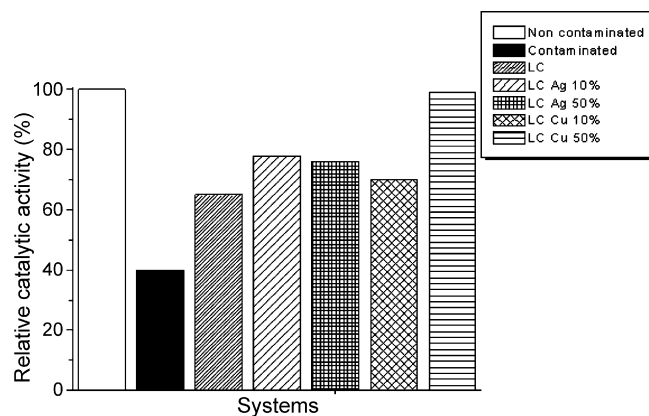


Fig. 7. Catalytic activity in the ethylene polymerization with $\text{TiCl}_4/\text{MgCl}_2$ catalyst, using cyclohexane contaminated with 50 ppm of acetone and percolated through chemically modified LC.

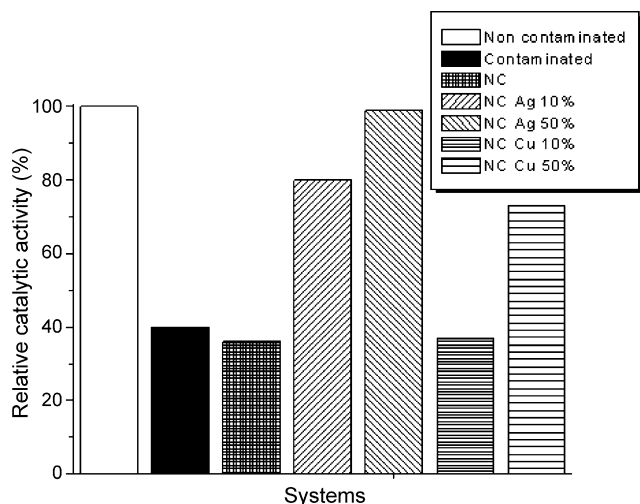


Fig. 8. Catalytic activity in the ethylene polymerization with $\text{TiCl}_4/\text{MgCl}_2$ catalyst, using cyclohexane contaminated with 50 ppm of acetone and percolated through chemically modified NC.

Table 6

Melting temperature (T_m) and crystallinity (X_c) of the polyethylene produced using solvent percolated by the different sorbents.

Systems	T_m (°C)	X_c (%)
Non-contaminated	133	45
Contaminated	133	43
S Cu 10%	133	56
LC Cu 50%	133	35
NC Ag 50%	133	49

mina [29]. The polymerization tests using NC modified with metal demonstrate that for this modification, Ag is more efficient. The higher the metal content in the adsorbent, the greater its efficiency in the acetone retention, which in turn, results in higher catalytic activity. The same occurs with LC modified with metals, in which higher metal content affords more efficient adsorbent. Cu improved the NC adsorbent capacity, but less than Ag. For modification with 50% metal in NC, Cu has 75% efficiency, as compared to 99% for Ag.

The resulting polyethylenes were characterized by DSC. In Table 6, the polymer melting points (T_m) and the crystallinities (X_c) of polymers produced by several systems are presented.

According to Table 6, the polymer melting points were typical of high-density polyethylene. No specific effect of the use of the adsorbent was evident in the crystallinity of the resulting polymers, which remained between 35 and 56%.

4. Conclusion

The addition of metal on silica and chrysotile can result in negative or positive effects on the acetone adsorption. This depends on the particular characteristics of the adsorbent, in terms of adsorbent nature, specific area, metal nature and metal content. The present results suggest that for acetone, retention in silica modified with 10% metal (Ag or Cu) is better. This content guarantees a favorable ratio between silanol groups and Lewis acid sites, both important components in acetone adsorption. For leached chrysotile, the acetone adsorption processes seem to be more complex. After acid treatment, leached chrysotile might become amorphous silica, and chemical modification with metals does not improve chrysotile adsorption capacity. However, this modification positively influenced the polymerization reactions, making this adsorbent a potential promoter in the system reaction. Yet, for leached and native chrysotile, higher metal addition percentages

lead to more efficient systems in acetone adsorption. Nevertheless, one cannot neglect that chrysotile asbestos fibers are associated to lung cancer or asbestosis mortality. Recently research has suggested that fibre dimension appears to be an important determinant of respiratory disease risk [30,31]. Therefore, the technological application of chrysotile as sorbent in polymerization plants may take into account safety procedures in order to eliminate its potential toxicological risks.

Acknowledgements

Gollmann thanks the UNIEMP Institute and Braskem for the grant. Mr. William Bretas Linares from SAMA is specially thanked for providing chrysotile samples. CNPq and FAPERGS/PRONEX are also thanked for partial support.

References

- [1] B.A. Krentzel, Y.V. Kissin, V.I. Kleiner, L.L. Stotskaya, *Polymers and Copolymers of Higher α -Olefins*, Hanser Publishers, Munich, 1997, p. 11.
- [2] Maak Business Services, *Polyethylene 2006*. World Congress, Zürich, Switzerland, February 21–22, 2006.
- [3] B. Chang, Y. Lu, B.J. Tatarchuck, Microfibrous entrapment catalyst or sorbent particulates for high contacting-efficiency removal of trace contaminants including CO and H₂S form practical reformats for PEM-H₂-O₂ fuel cells, *Chem. Eng. J.* 115 (2006) 195–202.
- [4] V. Kröger, U. Lassi, K. Kynkäänniemi, A. Suopanki, R.L. Keiski, Methodology development for laboratory-scale exhaust gas catalyst studies on phosphorus poisoning, *Chem. Eng. J.* 120 (2006) 113–118.
- [5] Y. Du, H. Chen, R. Chen, N. Xu, Poisoning effect of some nitrogen compounds on nano-sized nickel catalysts in *p*-nitrophenol hydrogenation, *Chem. Eng. J.* 125 (2006) 9–14.
- [6] D.D. Eley, C.H. Rochester, M.S. Scurrel, The polymerisation of ethylene on chromium oxide catalysts. III. An infrared study of the adsorption of carbon monoxide on active catalyst, *J. Catal.* 29 (1973) 20–30.
- [7] D.G.H. Ballard, D.R. Burnham, D.L. Twose, The measurement of the equilibrium constant for the formation of a complex between olefins and group IVA metal alkyls, *J. Catal.* 44 (1976) 116–125.
- [8] M.E. Grayson, M.P. McDaniel, Sulfide poisoning of ethylene polymerization over Philips Cr/Silica catalyst, *J. Mol. Catal. A: Chem.* 65 (1991) 139–144.
- [9] E.I. Vizen, L.A. Rishina, L.N. Sosnovskaja, F.S. Dyachkovsky, I.L. Dubnikova, T.A. Ladygina, Study of hydrogen effect in propylene polymerization on (with) the MgCl₂-supported Ziegler-Natta catalyst—Part 2. Effect of CS₂ on polymerization centres, *Eur. Polym. J.* 30 (1994) 1315–1318.
- [10] N.M. Ostrovskii, F. Kening, About mechanism and model of deactivation of Ziegler-Natta polymerization catalysts, *Chem. Eng. J.* 107 (2005) 73–77.
- [11] R.T. Yang, *Adsorbents. Fundamentals and Applications*, Wiley, New York, 2003.
- [12] I.B. Valentim, I. Joekes, Adsorption of sodium dodecylsulfate on chrysotile, *Colloid Surf. A: Physicochem. Eng. Aspects* 290 (2006) 106–111.
- [13] Y. Wan, C. Liu, The effect of humic acid on the adsorption of REEs on kaolin, *Colloid Surf. A: Physicochem. Eng. Aspects* 290 (2007) 112–117.
- [14] M.G. Fonseca, A.S. Oliveira, C. Airolidi, Silylating agents grafted onto silica derived from leached chrysotile, *J. Colloid Interf. Sci.* 240 (2001) 533–538.
- [15] C.F. Petry, L.B. Capeletti, F.C. Stedile, J.H.Z. dos Santos, D. Pozebon, Determination of titanium and vanadium in Ziegler-Natta catalysts by inductively coupled plasma atomic emission spectrometry, *Anal. Sci.* 22 (2006) 855–859.
- [16] R.P. Schwarzenbach, *Environmental Organic Chemistry*, Wiley, New York, 1995.
- [17] A. Morgan, R.J. Talbot, Acid leaching studies of neutron-irradiated chrysotile asbestos, *Ann. Occup. Hyg.* 41 (1997) 269–279.
- [18] El. Gazzano, E. Foresti, I.G. Lesci, M. Tomatis, C. Riganti, B. Fubini, N. Roveri, D. Ghigo, Different cellular responses evoked by natural and stoichiometric synthetic chrysotile asbestos, *Toxicol. Appl. Pharm.* 206 (2005) 356–364.
- [19] K. Liu, Q. Feng, Y. Yang, Y. Zhang, G.L. Ou, Y. Lu, Preparation and characterization of amorphous silica nanowires from natural chrysotile, *J. Non-Cryst. Sol.* 353 (2007) 1534–1539.
- [20] G. Larsen, S. Noriega, Dendrimer-mediated formation of Cu-Cu₂O nanoparticles on silica and their physical and catalytic characterization, *Appl. Catal. A: Gen.* 278 (2004) 73–81.
- [21] S. Cai, X. Xia, C. Xie, Research on Cu²⁺ transformations of Cu and its oxides particles with different sizes in the simulated uterine solution, *Corros. Sci.* 47 (2005) 1039–1047.
- [22] L. Núñez, E. Reguera, F. Corvo, E. González, C. Vazquez, Corrosion of copper in seawater and its aerosols in a tropical island, *Corros. Sci.* 47 (2005) 461–484.
- [23] W. Song, H. Jiu, O. Cong, B. Zhao, Silver microflowers and large spherical particles: controlled preparation and their wetting properties, *J. Colloid Interf. Sci.* 311 (2007) 456–460.
- [24] M.S. Ghattas, Sodium-hypophosphite as a novel reducing agent in the preparation and characterization of silver/silica gel catalysts, *J. Mol. Catal. A: Chem.* 248 (2006) 175–180.

- [25] A. Godec, U. Maver, M. Bele, O. Planinšek, S. Srčič, M. Gaberšček, J. Jamnik, Vitriification from solution in restricted space: formation and stabilization of amorphous nifedipine in a nanoporous silica xerogel carrier, *Int. J. Pharm.* 343 (2007) 131–140.
- [26] S. Lowell, J.E. Shields, M.A. Thomas, M. Thommes, *Characterization of Porous Solids and Powders: Surface Area, Pore Size and Density*, Kluwer Academic Publishers, Dordrecht, 2004.
- [27] E.F. Vansant, P. Van Der Voort, K.C. Vrancken, Characterization and modification of silica surface, *Stud. Surf. Sci. Catal.* 93 (1995) 65–75.
- [28] R.M. Silverstein, *Spectrometric Identification of Organic Compounds*, fifth ed., Wiley, New York, 1991.
- [29] M.A. Gollmann, L.B. Capeletti, J.H.Z. dos Santos, M.S.L. Miranda, Adsorbents for acetone from cyclohexane effluent, *Adsorption* 14 (2008) 805–813.
- [30] L. Stayner, E. Kuempel, S. Gilbert, M. Hein, J. Dement, Epidemiological study on the role of chrysotile asbestos fibre dimensions in determining respiratory disease risk in exposed workers, *Occup. Environ. Med.* 65 (2008) 613–619.
- [31] D.W. Berman, K.S. Crump, A meta-analysis of asbestos-related cancer risk that addresses fiber size and mineral type, *Crit. Rev. Toxicol.* 38 (2008) 49–73.